

Investigation of furan on vicinal Pd(1 1 1) by scanning tunneling microscopy

A. Loui, S. Chiang*

Department of Physics, University of California, Davis, California 95616-8677, USA

Available online 30 July 2004

Abstract

We have used scanning tunneling microscopy to image furan adsorbed on vicinal Pd(1 1 1) at temperatures below the onset of decomposition of the furan molecule. Studies conducted on two substrates with relatively narrow and wide terraces reveal strikingly different behaviors. Adsorbates on narrow vicinal planes are mobile at 225 K, while a scattered cluster distribution is observed on broader vicinal planes at comparable temperatures. Both surfaces exhibit upper step edges that are densely populated with furan molecules, which qualitatively match predicted STM images of furan generated from extended Hückel theory.

© 2004 Elsevier B.V. All rights reserved.

PACS: 68.43.Fg; 68.43.Hn; 68.37.Ef

Keywords: Scanning tunneling microscopy; Furan; Palladium; Adsorption; Low-index surfaces; Vicinal surfaces; Aromatic heterocompounds

1. Introduction

The study of heterogeneous catalysis is strongly motivated by the continuing need to produce, develop, and refine the petroleum-based fuels on which the industrialized world depends. Since crude oil reserves are finite, there has been a keen interest in alternative sources for carbon-containing feedstocks, including coal and biomass [1].

Oxygen-containing aromatic heterocompounds form the largest contaminant fraction in liquids derived from coal and biomass, with methylated phenols and furanic rings constituting the predominant species [1,2]. The presence of these compounds leads to issues of instability, since the contaminants react with air to form undesirable deposits [2]. Catalyzed removal of the oxygen heteroatom on late transition metals has been previously studied to some extent; for example, studies have been performed on the hydrodeoxygenation of furan (C_4H_4O) on reduced and sulfided Al_2O_3 -supported CoMo [3] and on carbon-supported NiMo and CoMo [4]. In contrast to these investigations, which were conducted under more

* Corresponding author. Tel.: +1 530 752 8538;
fax: +1 530 752 4717.

E-mail address: chiang@physics.ucdavis.edu (S. Chiang).

industrial conditions (e.g., 673 K at near atmospheric pressures of H₂ [3]) and on dispersed catalysts, model studies of furan on various single metal crystals under ultrahigh vacuum (UHV) conditions have shed light on the structure and orientation of the intact adsorbate [5–7] as well as provided details of the reaction mechanism on Pd(1 1 1) [8] and on O/Ag(1 1 0) [9].

We have used scanning tunneling microscopy (STM) to study furan adsorbed on the Pd(1 1 1) substrate in ultrahigh vacuum at temperatures below 280 K. This temperature corresponds to the threshold for the decomposition of the furan molecule, which has been studied by a variety of surface techniques [7,8,10]. In this paper, we will explore the surface structure of intact molecular overlayers. An STM study of the reaction above 280 K will be described in a future paper [11].

2. Experimental

The experiments were performed in an ultrahigh vacuum system (10^{-10} Torr base pressure) using an Oxford Instruments variable-temperature STM, which is part of a surface analysis system that also incorporates a low-energy electron microscope (LEEM) [12]. The Pd(1 1 1) single crystals were cleaned by repeated cycles of Ar⁺ ion bombardment and annealing to ~ 1000 K. Furan was purchased from Fisher Scientific (99+%, stabilized with 0.025–0.04% BHT) and further purified by multiple freeze–pump–thaw cycles to remove volatile contaminants. The clean Pd sample was precooled to 173–235 K (i.e., below the onset of furan decomposition) and then dosed with one Langmuir (L) (1×10^{-8} Torr for 100 s) of furan by back-filling the chamber via a variable leak valve. Purity of the gas-phase furan was verified by a quadrupole mass spectrometer prior to dosing. After allowing for thermal equilibration, the prepared sample was then imaged at the corresponding precooled temperature.

3. Results and discussion

Experiments utilized two stepped Pd(1 1 1) crystals, one with terraces of roughly 160–220 Å width (corresponding to about 0.8° miscut angle) and another of 20–45 Å width (corresponding to about

6.4° miscut angle). STM images of both pre-reaction surfaces show a subsaturation coverage of furan with no discernible long-range ordering. Calculations using the kinetic theory of gases and atomic van der Waals radii show that 1 L exposure at room temperature (300 K) yields coverages of roughly 5% of a monolayer and 28% of saturation, assuming a sticking coefficient of unity [6,13].

On the higher step density sample, the adsorbate features appear to populate large segments of the upper step edges. These features measure roughly 5–6 Å in diameter and generally appear to have a broad oval shape. Upon closer inspection, we can discern an asymmetric bi-lobed character to some of the features (Fig. 1). Comparison with theoretical images of flat-lying furan on high-symmetry binding sites on Pd(1 1 1), generated from semi-empirical Hückel molecular orbital theory, shows excellent qualitative correspondence with the observed features [14]. The experiment and theory, however, disagree on one detail: the minimum in the local density of states, predicted to lie along the molecular symmetry axis. This discrepancy can be due to insufficient resolution in the experimental image or inadequacy in the approximate Tersoff–Hamann perturbation theory on which the calculation is based [15,16].

The data suggest that the furan molecule is oriented with its aromatic ring parallel (or nearly parallel) to the Pd(1 1 1) crystallographic planes. Prior spectroscopic studies by Ormerod et al. utilizing high resolution electron energy loss and angle-resolved ultraviolet photoemission spectroscopies indicate that at least some fraction of the molecules are tilted with respect to the surface [7]. However, these data were obtained for saturation coverages corresponding to exposures at and in excess of 6 L [7]. We expect that the low coverages of furan in our experiments behave similarly to comparable coverages of benzene on Pd(1 1 1), in which the molecules assume a flat-lying configuration [17,18].

The asymmetry of the molecules, with a preponderance of Fermi-level electron density near the location of the oxygen heteroatom, allows us to distinguish two apparent orientations of furan along the upper step edge (Fig. 1c). The adsorbates appear to be largely adsorbed with the heteroatom facing in towards the terrace, with a smaller number rotated 180° outwards (approximate ratio of in:out is 4:1).

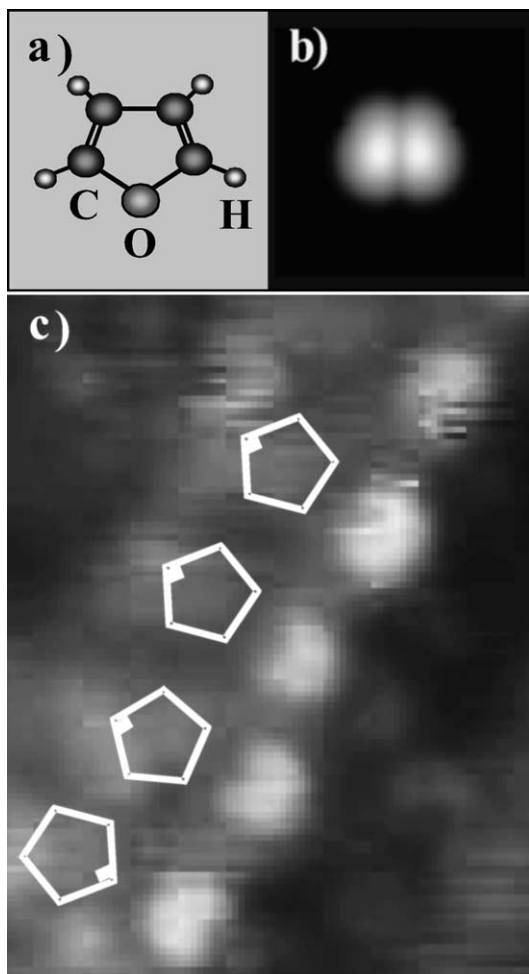


Fig. 1. (a) Schematic representation of furan molecule, with atomic species indicated. (b) Base 10 logarithmic plot of integrated Fermi-level electron density at 2 Å above molecular plane [14]. (c) 30 Å × 50 Å STM image of furan on Pd(1 1 1) at 225 K. The features populating the upper step edge are chiefly oriented with the heteroatom facing towards the terrace. Pentagons representing the furan molecule, with the oxygen atom marked, are added to guide the eye. Tunneling current is 0.13 nA, and sample bias is −1.0 V.

The terraces, however, are characterized by an indistinct corrugation (Fig. 2). In the vicinity of the upper step edges, oblong shapes appear which measure about 5 Å by 10 Å and are of lesser apparent height than the furan features located at the step edges (0.24 Å versus 0.56 Å). One likely explanation is that the adsorbates along the upper step edge are more strongly chemisorbed at their respective binding sites

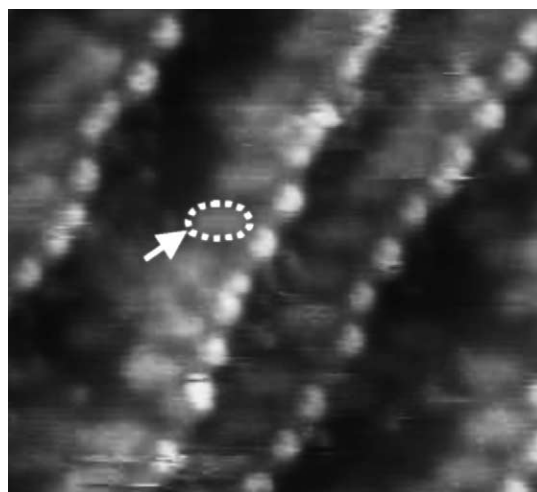


Fig. 2. 115 Å × 108 Å occupied states STM image of furan molecules on Pd(1 1 1) at 225 K. Furan populates the upper step edges, while the terraces show evidence of molecular diffusion. One of the broad, indistinct terrace features is indicated by an arrow. Tunneling current is 0.13 nA, and sample bias is −1.0 V.

than their terrace counterparts which, with appreciable translational diffusion rates, move too rapidly during the image acquisition time (82 s) to be observed. This phenomenon is commonly observed for subsaturation adsorbate coverages on late transition metal surfaces, from room temperature down to cryogenic conditions [19,20]. Examination of consecutive scans shows upper step edge features disappearing and appearing, presumably moving to and from the mobile terrace population; this is supported by the appearance of partially imaged features and streaky noise anomalies along the fast scan direction which persist for several lines (Fig. 3).

On the lower step density sample, a different pre-reaction distribution of intact furan molecules, each appearing as a single, bright oval feature, is observed (Fig. 4). The terrace features are scattered in small clusters containing roughly three to six molecules. These fill the entire width of the terraces up to the step edges. As with the higher step density sample, the upper step edges are completely populated with adsorbate features. Their overall shape and size (5–6 Å) correspond well to the previous data and the theoretical images. The surface feature density is estimated at 1.3×10^{14} molecules/cm²; this compares favorably to a density of 7.5×10^{13} molecules/cm² correspond-

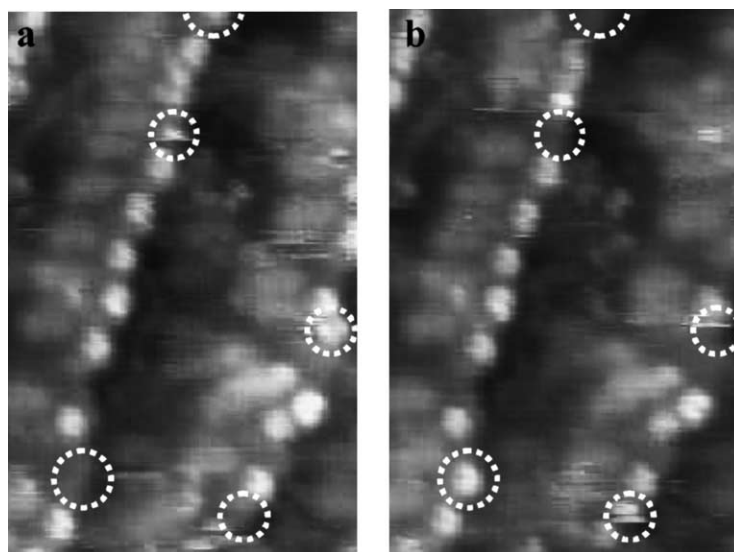


Fig. 3. Consecutive sequence (a and b) of $80 \text{ \AA} \times 120 \text{ \AA}$ STM images showing the disappearance and appearance of furan adsorbed along upper step edges at 225 K. Partially imaged features and streaky noise indicate translational diffusion, with the imaged adsorbates presumably moving to and from the mobile terrace population. The molecules which have moved between images (a and b) are indicated with open circles. Image acquisition time is 82 s. Tunneling current is 0.13 nA, and sample bias is -1.0 V .

ing to a 1 L exposure at 300 K, and suggests that the sticking coefficient is most likely near unity in value.

We speculate that the distribution of furan features for higher and lower step density samples is the result of the spatially dependent surface diffusion properties of the substrate. For the system of oxygen on Pt(1 1 1), preferential binding of molecules at the upper step edge has been inferred from STM observations at 300 K and *ab initio* local-density approximation calculations [21]. In addition, a study of CO on a highly stepped Pt(1 1 1) surface at 100 K found that upper step edges were populated exclusively for coverages up to 0.24 monolayers, with terrace adsorption proceeding at higher coverages to saturation [22]. Ma et al. [23] have measured surface diffusion coefficients for CO step-crossing on Pt(1 1 1). Based on their results and those of Ref. [21,22], they have suggested that the potential energy surface near the step is characterized by a Schwoebel–Ehrlich barrier at the lower step edge and a trapping potential well located at the upper step edge [23]. Such a model would support our observations of the distinct occupation of the upper step edges by $\text{C}_4\text{H}_4\text{O}$.

A plausible mechanism for the apparent difference in terrace adsorbate behavior is less obvious. We do

not believe that the small difference in temperature between the higher (225 K) and lower step density (199 K) data can explain the different molecular diffusion rates. In addition, at these temperatures, we would generally expect molecular diffusion to occur. Since the samples were prepared under identical conditions, this leaves the step density as the only possible explanation for the observed surface distribution behavior.

We speculate that the proximity of the upper and lower step edges for the higher step density surface may account for the differences in terrace behavior from the lower step density surface. Experimental studies of the self-diffusion of metal adatoms on metal vicinal surfaces [24–26] and theoretical calculations [27,28] have demonstrated that the surface potential behaves differently near the step edges, leading to regions that are only transiently occupied due to enhanced surface diffusion. This so-called “forbidden region” has been observed to be only twice the substrate nearest neighbor distance for single iridium adatoms on Ir(1 1 1) [24]. Given the narrow terrace widths of 20–45 Å on the higher step density sample, it is possible that such regions between the delimiting ascending and descending step edges could cover the

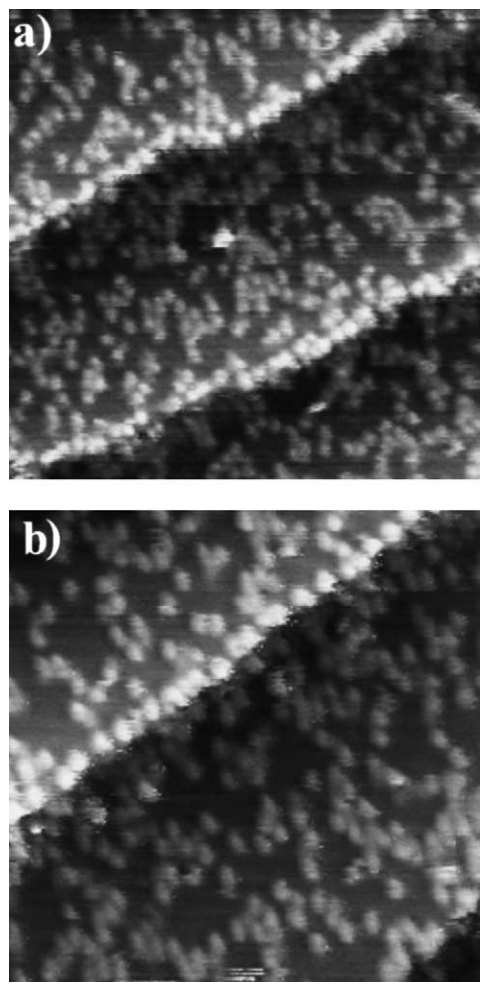


Fig. 4. Two STM images of furan on Pd(1 1 1) at 199 K, at different size scales under identical tunneling conditions (tunneling current is 0.2 nA and sample bias is -0.799 V). The submonolayer coverage is characterized by scattered adsorbate clusters containing roughly three to six molecules and a saturated upper step edge region. (a) Image size: $231 \text{ \AA} \times 231 \text{ \AA}$; (b) image size: $180 \text{ \AA} \times 180 \text{ \AA}$.

entire terrace for our molecular adsorbate system. An STM study of dilute benzene coverages on Cu(1 1 1) at 77 K reveals behavior similar to what we have observed in our system, with strongly bound species at the step edge region and evidence of diffusing molecules on the terraces [29]; here, transiently occupied regions are explained in terms of modulations in the local density of states created primarily by the step defect. Nevertheless, this model of the surface potential energy is not consistent with images of the lower

step density sample, on which no such “forbidden regions” can be seen. We note that a study of very dilute benzene coverages on stepped Ni(1 1 0) at 4 K showed evidence of *transient* molecular mobility, with a surface distribution very similar to what we have observed with furan on the higher step density Pd(1 1 1) substrate [30]. However, their experiments were deliberately focused on adsorbate motion well *below* the onset of the conventional, thermally activated diffusion which characterizes our system.

Future STM studies would first establish the threshold temperature for molecular motion and would then investigate the surface diffusion rates at higher temperatures on narrow vicinal planes from series of consecutive images. Based on the disappearance of features within the time interval of about six scan lines, and the assumption of travel over at least one molecular diameter (which corresponds to leaving the step edge region for the terrace), a linear diffusion speed of approximately 5 \AA/s is obtained from examining consecutive STM images at 225 K (Fig. 3). Another possible experiment involves the use of a linear optical diffraction method whereby surface diffusion is measured from the exponential decay of an adsorbate diffraction grating [31]. Angle-resolved diffusion studies on transition metal surfaces have been performed using this method [32,33]. Since this technique can measure diffusion rates up to thousands of \AA/s [34], furan adsorbed on the higher step density surface should be sufficiently mobile to be studied with this technique.

4. Conclusions

We have used STM to image furan adsorbed on stepped Pd(1 1 1) surfaces at temperatures below the onset of furan decomposition. Studies were conducted on two substrates, one with narrow vicinal planes (of $20\text{--}45 \text{ \AA}$ width) and another with relatively broader terraces ($160\text{--}220 \text{ \AA}$ width). Both surfaces show upper step edges saturated with adsorbate features, which qualitatively match predicted STM images of furan generated from extended Hückel molecular orbital theory. While the lower step density surface exhibits molecular clustering on its terraces, the higher step density surface shows evidence of a diffusing adsorbate population. Comparing the two substrates, the

only substantial difference is the step density, which we speculate gives rise to the observed surface diffusion properties. This conjecture is at least partially supported by models for adsorbate behavior near step edges on similar low Miller index metal surfaces.

Acknowledgements

We acknowledge partial funding support from the National Science Foundation (CHE-0111671). Acknowledgment is also made to the Donors of the American Chemical Society Petroleum Research Fund for partial support of this research.

References

- [1] E. Furimsky, *Appl. Catal. A* 199 (2000) 147.
- [2] E. Furimsky, *Catal. Rev. Sci. Eng.* 25 (1983) 421.
- [3] E. Furimsky, *Appl. Catal.* 6 (1983) 159.
- [4] K.V.R. Chary, K.S. Rama Rao, G. Muralidhar, P. Kanta Rao, *Carbon* 29 (1991) 478.
- [5] B.A. Sexton, *Surf. Sci.* 163 (1985) 99.
- [6] J.L. Solomon, R.J. Madix, J. Stöhr, *J. Chem. Phys.* 94 (1991) 4012.
- [7] R.M. Ormerod, C.J. Baddeley, C. Hardacre, R.M. Lambert, *Surf. Sci.* 360 (1996) 1.
- [8] T.E. Caldwell, I.M. Abdelrehim, D.P. Land, *J. Am. Chem. Soc.* 118 (1996) 907.
- [9] W.W. Crew, R.J. Madix, *J. Am. Chem. Soc.* 115 (1993) 729.
- [10] T.E. Caldwell, D.P. Land, *J. Phys. Chem. B* 103 (1999) 7869.
- [11] A. Loui, S. Chiang, manuscript in preparation.
- [12] C.L.H. Devlin, D.N. Futaba, A. Loui, J.D. Shine, S. Chiang, *Mat. Sci. Eng. B* 96 (2002) 215.
- [13] D.P. Woodruff, T.A. Delchar, *Modern Techniques of Surface Science*, Second ed., Cambridge University Press, Cambridge, 1994.
- [14] D.N. Futaba, S. Chiang, *J. Vac. Sci. Technol. A* 15 (1997) 1295.
- [15] J. Tersoff, D.R. Hamann, *Phys. Rev. Lett.* 50 (1983) 1998.
- [16] J. Tersoff, D.R. Hamann, *Phys. Rev. B* 31 (1985) 805.
- [17] H. Hoffmann, F. Zaera, R.M. Ormerod, R.M. Lambert, L.P. Wang, W.T. Tysoe, *Surf. Sci.* 232 (1990) 259.
- [18] W.T. Tysoe, R.M. Ormerod, R.M. Lambert, G. Zgrablich, A. Ramirez-Cuesta, *J. Phys. Chem.* 97 (1993) 3365.
- [19] V.M. Hallmark, S. Chiang, *Surf. Sci.* 286 (1993) 190.
- [20] J.C. Dunphy, M. Rose, S. Behler, D.F. Ogletree, M. Salmeron, *Phys. Rev. B* 57 (1998) 12705.
- [21] P.J. Feibelman, S. Esch, T. Michely, *Phys. Rev. Lett.* 77 (1996) 2257.
- [22] M.A. Henderson, A. Szabó, J.T. Yates, *J. Chem. Phys.* 91 (1989) 7245.
- [23] J. Ma, L. Cai, X.D. Xiao, M.M.T. Loy, *Surf. Sci.* 425 (1999) 131.
- [24] S.C. Wang, G. Ehrlich, *Phys. Rev. Lett.* 67 (1991) 2509.
- [25] S.C. Wang, G. Ehrlich, *Phys. Rev. Lett.* 70 (1993) 41.
- [26] K. Kyuno, G. Ehrlich, *Phys. Rev. Lett.* 81 (1998) 5592.
- [27] C.-L. Liu, J.B. Adams, *Surf. Sci.* 294 (1993) 197.
- [28] S. Liu, H. Metiu, *Surf. Sci.* 359 (1996) 245.
- [29] S.J. Stranick, M.M. Kamna, P.S. Weiss, *Surf. Sci.* 338 (1995) 41.
- [30] J.H. Ferris, J.G. Kushmerick, J.A. Johnson, P.S. Weiss, *Surf. Sci.* 446 (2000) 112.
- [31] X.D. Zhu, Th. Rasing, Y.R. Shen, *Phys. Rev. Lett.* 61 (1988) 2883.
- [32] E. Nabighian, X.D. Zhu, *Phys. Rev. B* 58 (1998) 7552.
- [33] X.D. Xiao, X.D. Zhu, W. Daum, Y.R. Shen, *Phys. Rev. Lett.* 66 (1991) 2352.
- [34] X.D. Zhu, private communication.